Solving Surface Structures with X-Ray Diffraction

Robert Feidenhans'l, Jakob Bohr*, Mourits Nielsen, Michael Toney**
Risø National Laboratory, DK-4000 Roskilde, Denmark

Robert L. Johnson, Francois Grey
Max-Planck-Institut für Festkörperforschung, D-7000 Stuttgart, Federal Republic of Germany

Ian K. Robinson
AT&T Bell Laboratories, Murray Hill, NJ 07974, USA

Summary: Despite much effort, the detailed atomic structure of most surfaces is still not known. This paper reviews the recent developments in using X-ray diffraction for studying surfaces. Experiments on InSb(111)2×2 are discussed as an example of how to solve surface structures by Fourier methods, without any a priori model.

1 Introduction

Diffraction studies of surface structures are usually done with Low Energy Electron Diffraction (LEED). The great surface sensitivity of LEED is due to the strong interaction between electrons and matter which, however, causes multiple scattering effects that inhibit a simple interpretation of experimental results. Thus, in spite of the amount of work done with LEED, most surface structures remain unsolved.

X-ray diffraction, on the other hand, has the simplicity of interpretation needed but X-rays interact weakly with matter and therefore the technique is normally not surface sensitive. But through the development of intense X-ray sources such as synchrotrons and the use of grazing angles of incidence, the surface signal can be enhanced considerably, and X-ray diffraction is becoming an important tool in surface science.

Applying a kinematical scattering theory, the structure factor amplitudes are easily calculated from the experimental data and the classical methods of crystallography, such as the Patterson function or the error synthesis, can be used in favourable

* Present address: Brookhaven Nat. Lab., Upton, N.Y. 11973, USA.
** Permanent address: IBM Research Lab., San Jose, CA 95193, USA.

cases to solve the structure in an elegant way. A number of studies have already been made, mainly on clean surface reconstructions: Ge(100)2×1 [1], Au(110) 2×1 [2], InSb(111)2×2 [3], Si(111)7×7 [4] and also on an adsorbate system Pb on Cu(110) [5], showing the possibilities of the new technique.

2 Theory of Grazing Angle Incidence Technique

Consider X-rays entering a continuous medium and assume the interface between the medium and vacuum to be sharp. It is then straightforward from the Fresnel formulae [6] to calculate the electric field vectors for the reflected and refracted wave. Assume an incoming plane wave with the electric field vector $\vec{E}$ and let $\vec{E}'$ and $\vec{E}''$ be the electric field vectors of the reflected and refracted waves, respectively.

The calculation and formulae for $\vec{E}'$ and $\vec{E}''$ are given in [7], we will only discuss the results qualitatively. The refractive index n is given by (neglecting absorption):

$$n = 1 - \delta \tag{1}$$

$$\delta = \frac{N_0 e^2}{2\pi mc^2} \frac{Z\rho}{A} \lambda^2 \quad \text{(c.g.s. units)} \tag{2}$$

N_0 is Avogadro's number, Z the atomic number of the medium, A the mass number, ρ the electron density and λ the wavelength of the incoming X-rays. Because the refractive index n is less than one, total external reflection ($|\vec{E}| = |\vec{E}'|$), will occur for incident angles θ less than or equal to a critical angle $\theta_c = (2\delta)^{1/2}$. Typically δ is of the order 10^{-6}, so θ_c will be in the range $0.2° \ldots 0.5°$ for wavelengths of about 1.5 Å. The wavevector $\vec{k}''$ of the refracted wave $\vec{E}''$ is calculated to have an imaginary component perpendicular to the surface for $\theta < \theta_c$. It means that the refracted wave is propagating parallel to the surface while being exponentially damped in the medium, even in the limit of no absorption. It is this wave that is involved in the diffraction from the surface lattice. Moreover, the amplitude of $|\vec{E}''|$ at the surface has a maximum at $\theta = \theta_c$. In the limit of no absorption $|\vec{E}''| = 2|\vec{E}|$ for $\theta = \theta_c$. This, in combination with the exponential damping perpendicular to the surface, is what makes X-rays surface sensitive. The 1/e length for the damping perpendicular to surface and the intensity of the refracted wave normalized to the incoming wave ($(|\vec{E}''|/|\vec{E}|)^2$) are shown, as a function of angle of incidence θ in Fig. 1a and 1b, respectively, in the specific case of an InSb($\overline{111}$)B surface with $\lambda = 1.2$ Å and including absorption.

3 Experiment

Since in surface diffraction experiments only about 10^{15} atoms/cm^2 are contributing to the scattering intensity the most intense X-ray sources are needed, meaning that we must combine synchrotron X-ray diffraction with the UHV technique man-

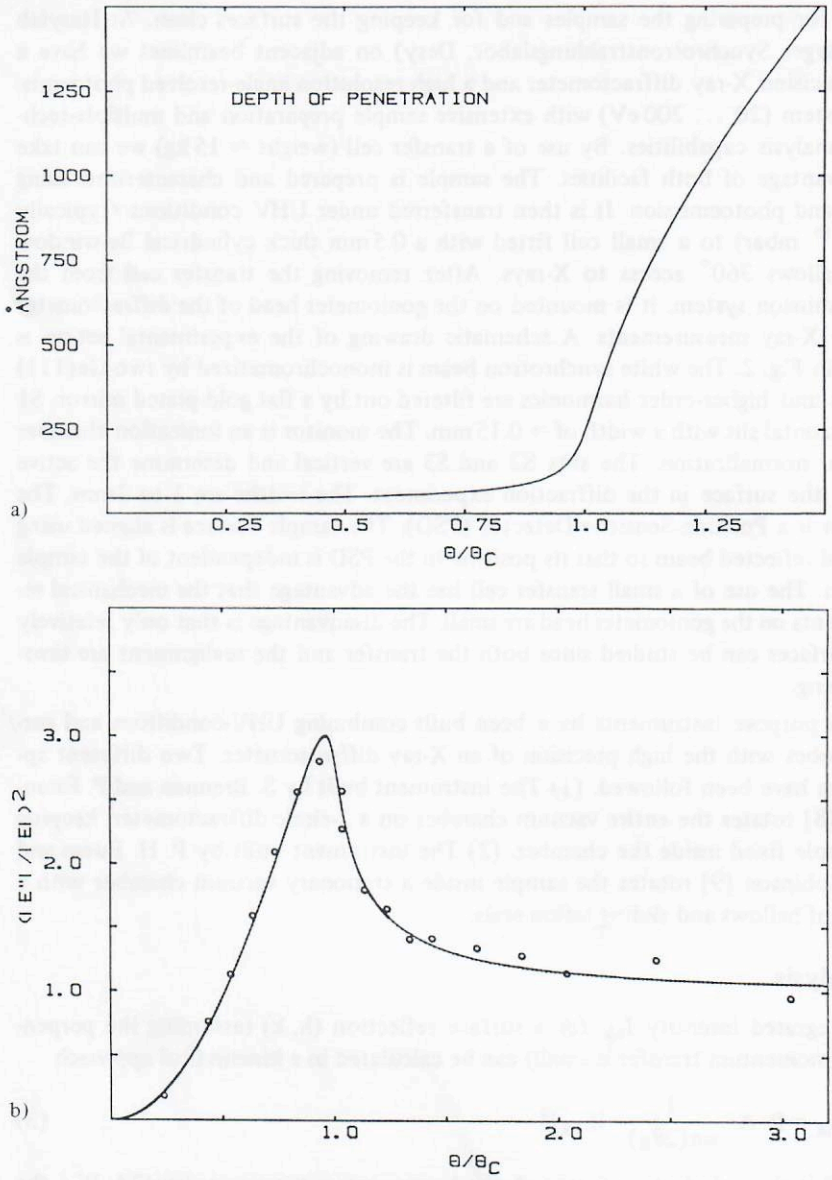

Fig. 1 (a) The 1/e depth of penetration perpendicular to the surface is shown as a function of the angle of incidence θ.

(b) The intensity of the refracted wave as function of the angle of incidence θ.

The curves are shown for a InSb (111) surface with a wavelength of $\lambda = 1.2$ Å, the critical angle $\theta_c = 0.25°$. The experimental points in (b) are from the (4/3,0) reflection of the InSb $(\overline{111})$B 3×3 surface normalized to the correct scale.

datory for preparing the samples and for keeping the surfaces clean. At Hasylab (Hamburger Synchrotronstrahlungslabor, Desy) on adjacent beamlines we have a high precision X-ray diffractometer and a high resolution angle-resolved photoemission system (20 ... 200 eV) with extensive sample preparation and multiple-technique analysis capabilities. By use of a transfer cell (weight $\approx$ 15 kg) we can take full advantage of both facilities. The sample is prepared and characterized using LEED and photoemission. It is then transferred under UHV conditions (typically 2×10^{-10} mbar) to a small cell fitted with a 0.5 mm thick cylindrical Be-window which allows 360° access to X-rays. After removing the transfer cell from the photoemission system, it is mounted on the goniometer head of the diffractometer for the X-ray measurements. A schematic drawing of the experimental set-up is shown in Fig. 2. The white synchrotron beam is monochromatized by two Ge(111) crystals and higher-order harmonics are filtered out by a flat gold-plated mirror. S1 is a horizontal slit with a width of $\approx$ 0.15 mm. The monitor is an ionization chamber used for normalization. The slits S2 and S3 are vertical and determine the active area of the surface in the diffraction experiment. The widths are 1 to 2 mm. The detector is a Position-Sensitive-Detector (PSD). The sample surface is aligned using the total reflected beam so that its position in the PSD is independent of the sample rotation. The use of a small transfer cell has the advantage that the mechanical requirements on the goniometer head are small. The disadvantage is that only relatively inert surfaces can be studied since both the transfer and the realignment are time-consuming.

General purpose instruments have been built combining UHV-conditions and surface probes with the high precision of an X-ray diffractometer. Two different approaches have been followed. (1) The instrument built by S. Brennan and P. Eisenberger [8] rotates the entire vacuum chamber on a 2-circle diffractometer, keeping the sample fixed inside the chamber. (2) The instrument built by P. H. Fuoss and I. K. Robinson [9] rotates the sample inside a stationary vacuum chamber with a system of bellows and sliding teflon seals.

4 Analysis

The integrated intensity I_{hk} for a surface reflection (h, k) (assuming the perpendicular momentum transfer is small) can be calculated in a kinematical approach

$$I_{hk} \sim P \cdot A \cdot \frac{1}{\sin(2\theta_B)} \cdot |F_{hk}|^2 \tag{3}$$

where P is the polarization factor, A the beam cross-section area, $(\sin(2\theta_B))^{-1}$ the Lorentz factor with the Bragg angle θ_B. F_{hk} is the structure factor containing the information about the atomic geometry and is given by

$$F_{hk} = \sum_{j=1}^{N} f_j(h,k)\, e^{-M_j}\, e^{2\pi i(hx_j + ky_j)} \tag{4}$$

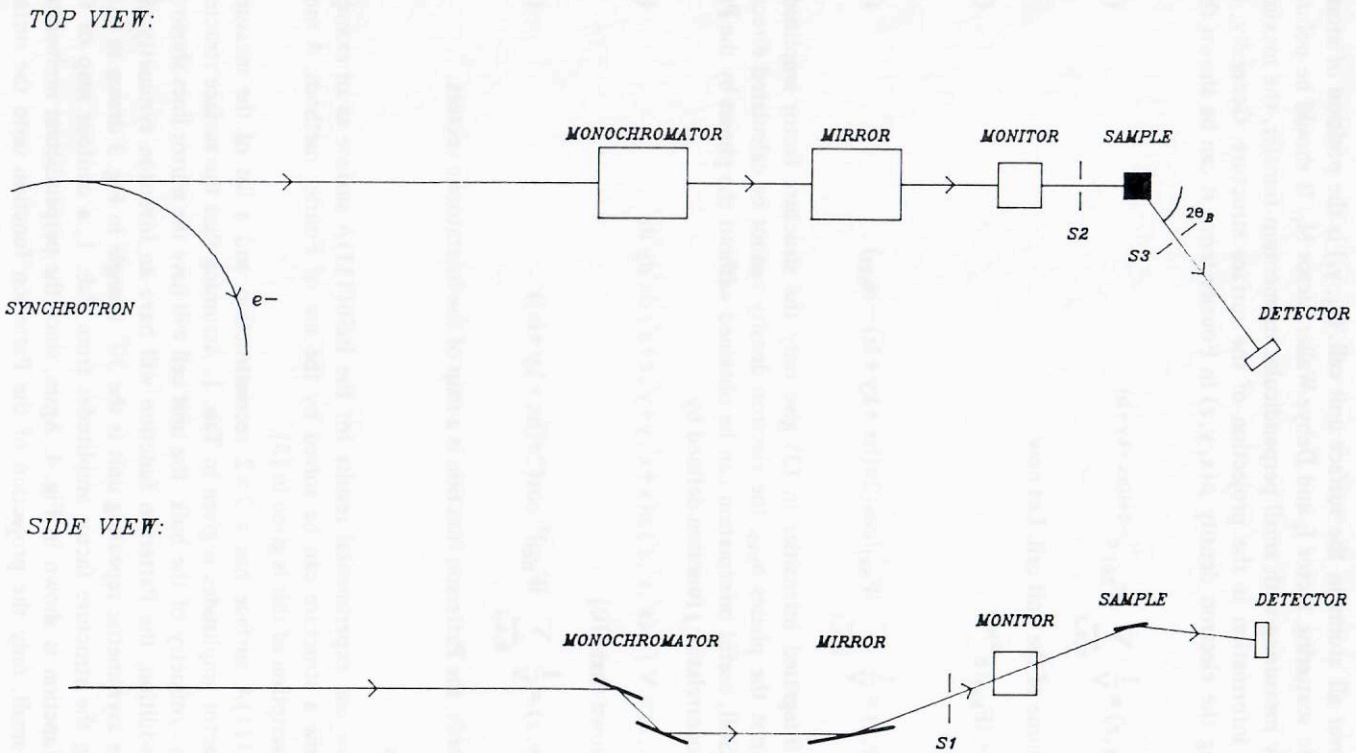

Fig. 2 Schematic drawing of the experimental set-up. Lengths and angles are not to scale. For explanation see text. In this arrangement the polarization factor is $P = \cos^2(2\theta_B)$ and the active area $A \sim 1/\sin(2\theta_B)$.

summing over all atoms in the surface unit cell. (x_j, y_j) is the position of atom j with atomic scattering factor f_j and Debye-Waller factor M_j. It should be pointed out that by measuring with small perpendicular momentum transfer, the maximal obtainable information is the projection of the surface structure. Generally, by representing the electron density $\rho(x, y, z)$ in Fourier terms it can be shown that [10]

$$\rho(x,y,z) = \frac{1}{V} \sum_{h,k,l} F_{hkl}\, e^{-2\pi i(hx+ky+lz)} \tag{5}$$

V is the volume of the unit cell. Let now

$$F_{hkl} = |F_{hkl}|\, e^{i\alpha_{hkl}} \ . \tag{6}$$

Then

$$\rho(x,y,z) = \frac{1}{V} \sum_{h,k,l} |F_{hkl}| \cos(2\pi(hx+ky+lz) - \alpha_{hkl}) \ . \tag{7}$$

Since the integrated intensities in (3) give only the structure factor amplitudes $|F_{hkl}|$ and not the phases α_{hkl}, the electron density cannot be calculated directly from I_{hkl}. Still, useful information can be obtained without the phases by the Patterson (autocorrelation) function defined by

$$P(x,y,z) = V \int \rho(x',y',z')\, \rho(x+x', y+y', z+z')\, dx'dy'dz' \ . \tag{8}$$

It can be shown that [10]

$$P(x,y,z) = \frac{1}{V} \sum_{h,k,l} |F_{hkl}|^2 \cos(2\pi(hx+ky+lz)) \ . \tag{9}$$

In other words, the Patterson function is a map of the interatomic vectors.

5 Results

We will now use experimental results for the InSb(111)A surface as an example to show how a structure can be solved by the use of Fourier methods. A more detailed description of this is given in [3].

The InSb(111)A surface has a 2×2 reconstruction and a list of the measured structure factor amplitudes is given in Tab. 1. Assuming that the surface structure has the 3m symmetry of the bulk, the unit cell will have the mirror lines shown in Fig. 3. In addition, the Patterson function will have an inversion symmetry (see (9)), so the asymmetric repeating unit is the 30° triangle in Fig. 3 drawn in thick lines. Using the structure factor amplitudes from Tab. 1, a contour map of the Patterson function is shown in Fig. 4. Again, since the perpendicular momentum transfer is small, only the projection of the Patterson function onto the surface

Table 1 Observed and calculated surface structure amplitudes for InSb(111) 2 × 2. The indices (h, k) used to label the reflections refer to the hexagonal coordinate frame defined in Fig. 3. (6) refers to the values calculated for the 6 atom model derived directly from the Patterson after adjustment of a scale factor only. (7) refers to the final 4 parameter model. From Ref. [3].

H	k	F_{hk}^{obs}	$F_{hk}^{calc(6)}$	$F_{hk}^{calc(7)}$
1/2	0	3.5 ± .2	9.0	4.0
1/2	1/2	6.2 ± .5	9.4	6.4
1	1/2	21.1 ± .4	10.0	21.0
3/2	0	32.1 ± .6	30.0	31.6
3/2	1/2	8.6 ± .5	3.1	9.0
3/2	1	7.6 ± .5	13.8	8.0
3/2	3/2	9.3 ± 1.0	11.3	11.6
2	1/2	18.5 ± .9	15.9	19.0
2	3/2	17.5 ± .8	9.3	17.3
5/2	0	26.2 ± 1.1	14.6	22.0
5/2	1/2	16.6 ± 1.0	5.2	17.5
5/2	1	29.4 ± 1.2	26.5	29.2
5/2	3/2	14.1 ± .8	9.0	14.7
3	1/2	3.8 ± 2.6	4.1	2.6
7/2	0	8.9 ± 2.2	12.2	9.1
7/2	1/2	12.8 ± 2.0	12.6	13.7

plane is obtained. One more comment should be made. As can be seen from Tab. 1 only fractional order reflections are measured. The reason is that scattering from the bulk may influence the intensity of the integer-order reflections. The omission of the integer-order reflections can of course distort the Patterson function.

There are three clear non-origin peaks in the Patterson that must correspond to interatomic vectors in the surface structure. The bulk structure projected onto the surface plane is a honeycomb arrangement of atoms, in which the repeating unit is a hexagon, shown as open circles in Fig. 4(b). If the hexagon is placed in a 2 × 2

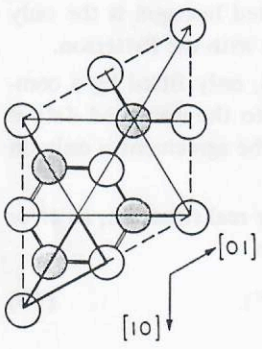

Fig. 3

The unit cell for the InSb (111)A 2 × 2 surface. The full lines shown are the mirror lines of 3m symmetry and the 30° triangle (thick lines) is the asymmetric repeating unit in the Patterson function, see Fig. 4. The hexagonal unit cell vectors shown are used and defined:

$[1,0]_{hex} = [1/2, -1/2, 0]_{bulk}$ and $[0,1]_{hex} = [0,1/2, -1/2]_{bulk}$.

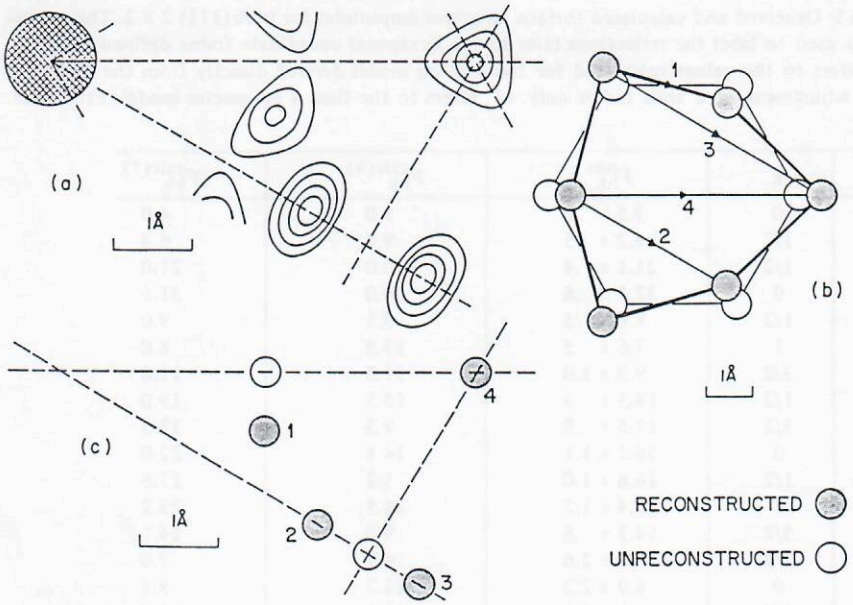

Fig. 4 (a) Repeating unit of the Patterson function calculated for the F_{hk}^{obs} in Tab. 1. Positive contour levels above zero are shown. The dashed lines are mirror lines and the shaded circle is the origin peak rising 17 contour levels.

(b) Distortion of a hexagonal arrangement of atoms taken from the projected unreconstructed InSb (111) surface.

(c) Pair-correlation peaks 1 to 4 derived from vectors 1 to 4 in (b). From Ref. [3].

unit cell, the interatomic vectors are the open circles shown in Fig. 4(c). If the hexagon is distorted conserving bondlengths, as the closed circles in Fig. 4(b) show, the peaks in the Patterson function move to the positions indicated in 4(c), which are exactly those observed in 4(a). The distorted hexagon is the only simple arrangement of atoms with 3m symmetry that agrees with the Patterson.

The structure factors calculated for the distorted hexagon, only fitted by a common scale factor, are given in Tab. 1, but the agreement to the measured data is poor. The mean square residual is $\chi^2 = 125$, meaning that the agreement is only on a ten-standard-deviation level.

However, assuming that the distorted hexagon is close to the real structure, an error synthesis or difference electron density map $\Delta\rho$ can be made

$$\Delta\rho(x,y) = \sum_{h,k} (F_{hk}^{obs} - |F_{hk}^{calc}|) \cos(2\pi(hx + ky) - \alpha_{hk}^{calc}). \qquad (10)$$

A positive peak in $\Delta\rho$ indicates an atom not included, a negative peak indicates one too many. The assumption made is that the phases for the model structure are close to phases for the real structure.

The contour map of $\Delta\rho$ is shown in Fig. 5. A single peak, well above the noise level of the map, indicates a seventh atom on one of the three-fold axes. The seven-

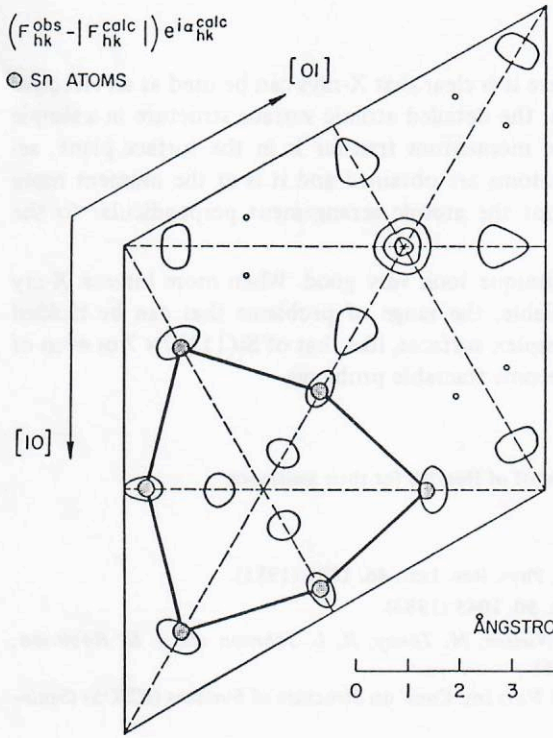

Fig. 5
Difference Fourier map of one InSb (111) 2 × 2 unit cell. Positive contours above zero are shown. Calculated coefficients $F_{hk}^{calc(6)}$ in Tab. 1 are derived from the distorted hexagon of Sn atoms shown. From Ref. [3].

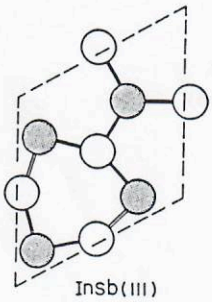

Fig. 6
Final structure for InSb (111) A 2 × 2 surface. The Sb atoms are shaded. The outward radial displacement of the three Sb atoms is (0.45 ± 0.04) Å and the inward radial displacement of the three In atoms is (0.23 ± 0.05) Å. The overall temperature factor corresponds to a one component vibrational amplitude of 0.12 Å. From Ref. [3].

atom structure has a residual of $\chi^2 = 25$ which drops to 2.1 when the positions are least-square refined, and a thermal parameter is included. The calculation above has been made assuming all atoms to be Sn. Assigning atoms to be either In or Sb, the best agreement is made with three In and four Sb atoms, meaning a vacant In site. This structure is shown in Fig. 6. The structure factors for the final model are given in Tab. 1. It should be stressed that the structure was solved without assuming any a priori model.

6 Conclusions

From the example mentioned here it is clear that X-rays can be used as an effective surface sensitive probe to unravel the detailed atomic surface structure in a simple way. Since the main part of the momentum transfer is in the surface plane, accurate in-plane positions of the atoms are obtained and it is at the moment more difficult to get information about the atomic arrangement perpendicular to the surface.

The future prospects of the technique look very good. When more intense X-ray synchrotron beams become available, the range of problems that can be tackled will increase and much more complex surfaces, like that of Si(111)7×7 or even of a biological membrane, should become tractable problems.

Acknowledgements

We wish to express our thanks to the staff of Hasylab for their assistance.

References

[1] *P. Eisenberger* and *W. C. Marra*, Phys. Rev. Lett. **46**, 1081 (1981).

[2] *I. K. Robinson*, Phys. Rev. Lett. **50**, 1045 (1983).

[3] *J. Bohr, R. Feidenhans'l, M. Nielsen, M. Toney, R. L. Johnson* and *I. K. Robinson*, Phys. Rev. Lett. **54**, 1275 (1985).

[4] *I. K. Robinson*, Proceedings of First Int. Conf. on Structure of Surfaces (ICSOS) (Springer 1984).

[5] *W. C. Marra, P. H. Fuoss* and *P. Eisenberger*, Phys. Rev. Lett. **49**, 1169 (1982).

[6] *M. Born* and *E. Wolf*, Principles of Optics (Pergamon Press, New York 1983).

[7] *G. H. Vineyard*, Phys. Rev. **B26**, 4146 (1982).

[8] *S. Brennan* and *P. Eisenberger*, Nucl. Instr. Meth. **222A**, 164 (1984).

[9] *P. H. Fuoss* and *I. K. Robinson*, Nucl. Instr. Meth. **222A**, 171 (1984).

[10] *B. E. Warren*, X-ray Diffraction (Addison-Wesley, Reading, Mass, 1968).